Decoupling mobility and charge carrier concentration in AgR-$AgPO_3$ glasses (R = Cl, Br, I)

Bruno P. Rodrigues[1,2]*, Heike Ebendorff-Heidepriem[2], Lothar Wondraczek[1,3]

[1]*Otto Schott Institute of Materials Research, Friedrich Schiller University of Jena, Fraunhoferstr. 6 07743 Jena, Germany*

[2]*Institute of Photonics and Advanced Sensing, School of Physical Sciences, ARC Centre of Excellence for Nanoscale BioPhotonics, The University of Adelaide, SA 5005, Australia*

[3]*Center of Energy and Environmental Chemistry, University of Jena, Philosophenweg 7, 07743 Jena, Germany*

*bruno.polettorodrigues@adelaide.edu.au

ABSTRACT

Halide-containing silver phosphate glasses have been used as model systems for the study of the ionic conductivity of oxide glasses for the past 50 years, mostly due to the massive increase in conductivity observed as the halide concentration is increased, even if the molar ratio of silver is kept constant. Furthermore there is still no consensus if the increased conductivity is due to an enhancement of the number of effective charge carriers (glass as a weak electrolyte) or a higher charge carrier mobility (glass as a strong electrolyte). In this work we investigate the electrical properties of silver-halide-containing silver metaphosphate glasses through Impedance Spectroscopy. We find the glasses to follow the “canonical scaling”, which coupled with the diffusional nature of the conductivity allows us to show that the number of effective charge carriers remains constant with increasing halide concentration, and that the conductivity follows the same scaling as the ionic mobility.

I. INTRODUCTION

In the past decades, ion conducting amorphous materials have attracted a great deal of both academic and industrial interest. Even to this day, however, there is no widely accepted model of ion transport in disordered media, all the while the horizon of potential applications keeps broadening[1–6]. Since the first experimental reports on salt-doped metaphosphates from the

late 1970's[7–9], this family of glasses has been under investigation; especially because metaphosphates can be combined with high molar concentrations of halides, sulphides, and sulphates while maintaining reasonable glass forming ability[7,8,10–16], and the addition of such salts increases the measured ionic conductivity by several orders of magnitude. The prime example of such behaviour is the silver metaphosphates doped with silver iodide, where the addition of 50 mol% of AgI increases the conductivity at room temperature by 6 orders of magnitude in comparison with the pure silver metaphosphate, with very little change in the number density of silver atoms, and therefore, of charge carriers[9,17]. Early studies[18–21] proposed that the observed increase in conductivity was due to the presence of α-AgI clusters embedded between the phosphate chains, since crystalline silver iodide is itself a superionic silver conductor; however recent structural (especially NMR) studies[22–25] have shown that the iodide ion is homogeneously distributed in the Ag^+ coordination spheres, leading to an increased average separation between the phosphate chains but otherwise keeping the phosphate short-range order intact[26].

The direct-current conductivity of single, monovalent ion conducing materials in $\Omega^{-1}.m^{-1}$ can be written, in its most basic form[4,9], as:

$$\sigma_{\mathrm{dc}} = n.e.\mu \qquad 1$$

where n is the number density of effective charge carriers given by $n = \gamma.n_c$ with γ being the fraction of charge carriers that are mobile and n_c is the total number density of ions, e is the elementary charge and μ is the charge carrier mobility. While this expression contains the key factors describing the conductivity, it is challenging to decouple the compositional effects in the mobility and charge carrier density so as to clarify which of the two dominates the material's properties[27–30]. Therefore one finds in the literature two different interpretations of the influence of the salt doping in phosphate glasses[9]: the "weak-electrolyte" approach posits that the enhancement in conductivity is due to an increase in the fraction of effective charge carriers[7,11,17,19,31–33] (for example, Rodrigues *et al*. report an increase of approximately 5 orders

of magnitude in γ by adding AgI to $AgPO_3$ glasses[17]) while the ionic mobility is practically composition independent (Clement *et al*. report a value of 6 x 10^{-4} $cm^2.V^{-1}.s^{-1}$ at room temperature, independent of silver iodide content in AgI-$AgPO_3$ glasses[34]); alternatively, according to the "strong-electrolyte" model, the augment in conductivity is rooted in increased charge carrier mobility, since $\gamma \sim 1$[2,3,35–38].

The Walden rule is an empirical relation proposed in the early 1900's, stating that, for an ion-conducting liquid, the product of the molar conductivity $\Lambda = \sigma \cdot V_m$ (where V_m is the molar volume) and its viscosity η is constant[39]:

$$\Lambda \cdot \eta = \text{constant} \qquad 2$$

This relation is a natural consequence from the observation that in diluted electrolyte solutions with weakly-interacting ions, the ionic mobility is controlled by ionic diffusion in the solvent. Formulated alternatively, the diffusion coefficient related to the conductivity D_σ according to the Nernst-Einstein relation is equal to the viscosity diffusion coefficient D_η as given by the Stokes-Einstein relation[40].

$$D_\sigma = \frac{\sigma_{\mathrm{dc}} \cdot k \cdot T \cdot H_R}{\gamma \cdot n_c \cdot e^2} \qquad 3$$

$$D_\eta = \frac{k \cdot T}{g \cdot \eta \cdot r} \qquad 4$$

where k is Boltzmann's constant, T is the absolute temperature, H_R is the Haven Ratio[41,42], g is a geometrical factor (equal to 6π[40]) and r is the ionic radius. So, if $D_\sigma = D_\eta$:

$$\frac{\sigma_{\mathrm{dc}} \cdot k \cdot T \cdot H_R}{\gamma \cdot n_c \cdot e^2} = \frac{k \cdot T}{g \cdot \eta \cdot r} \qquad 5$$

$$\sigma_{\mathrm{dc}} \cdot \eta = \frac{\gamma \cdot n_c \cdot e^2}{g \cdot r \cdot H_R} = C \qquad 6$$

from which we recover the original Walden rule (**Equation 2**) by substituting $\sigma_{dc} = \Lambda/V_m$. Following **Equation 6**, the Walden plot ($\log(\Lambda) \times \log\eta^{-1}$) is proven helpful in assessing the "ionicity" of ionic liquids. If a liquid can be treated as an ensemble of independent ions and there are no ion-ion interactions, it should exhibit a slope of one. Deviations from this ideal case enables the detection of different forms of ion-matrix interactions[40,43–45], and can be described by the so-called *fractional Walden Rule* $\Lambda \cdot \eta^{\alpha} = \text{constant}$ (with $\alpha < 1$). Such deviations can also be understood in terms of the "decoupling index" $R = \langle\tau_s\rangle/\langle\tau_\sigma\rangle$, defined as the ratio between the structural and conductivity relaxation times[46,47].

In analogy, the same reasoning can be applied to the case where the ionic conductivity is instead controlled by the random hopping of charge carriers. In the case of Brownian motion, the self-diffusion coefficient of an ion is given by the Einstein formula[27,48].

$$D_i^* = \frac{\langle x^2(t^*)\rangle}{g' \cdot t^*} \qquad 7$$

where$\langle x^2(t^*)\rangle$ is the mean-squared displacement at a characteristic time-scale t^* and g' is a geometrical constant (equal to 6 for an isotropic cubic lattice). For ion-conducting materials, the diffusive motion between neighbouring equilibrium positions where ions become "trapped"[41,49] occurs in a time-scale $t = 1/\Gamma$ related to the onset of the dispersive regime of conductivity[50–53]. For such materials, the distance between trapping sites can be approximated by the average distance between ions d[53], so **Equation 7** can be rewritten as:

$$D_i = \frac{d^2 \cdot \Gamma}{g'} \qquad 8$$

Therefore, if $D_\sigma = D_i$:

$$\frac{\sigma_{\mathrm{dc}} \cdot k \cdot T \cdot H_R}{\gamma \cdot n_c \cdot e^2} = \frac{d^2 \cdot \Gamma}{g'} \qquad 9$$

$$\frac{\sigma_{\mathrm{dc}} \cdot T}{\Gamma} = \frac{\gamma \cdot d^2 \cdot n_c \cdot e^2}{g' \cdot k \cdot H_R} = C' \qquad 10$$

Similarly to **Equation 6**, **Equation 10** describes a slope of unity in a $\log(\sigma_{\mathrm{dc}} \cdot T) \times \log \Gamma$ graph, which is indicative of materials whose conductivity is controlled by ionic hopping, and, in parallel with the Walden rule for ionic liquids, also imply the material can be understood as a random mixture of ions where the ion-ion correlations are negligible. This is equivalent to the so-called "canonical scaling" when applied to the analysis of the frequency dependence of the real part of the conductivity $\sigma'(f)$. This relation is expected to hold independently of temperature if the matrix remains isostructural[54]. Another feature of **Equations 6** and **10** is that the constants C and C' (and, therefore, the intercepts in the $\log(\Lambda) \times \log \eta^{-1}$ and $\log(\sigma_{\mathrm{dc}} \cdot T) \times \log \Gamma$ graphs) are proportional to the number of effective charge carriers. Consequently, an increase in the number of effective charge carriers should result in an upward shift of the data along the $\log(\Lambda)$- or the $\log(\sigma_{\mathrm{dc}} \cdot T)$-axis (if **Equation 6** or **10** are graphed, respectively). Such effect has been reported, for example, for ionic liquids with increasing pK_a[44], and for thioborate glasses with increasing alkali content[54].

Based on this analysis, we investigate the electrical properties of silver halide – silver metaphosphate glasses by impedance spectroscopy and attempt to elucidate if the measured enhancement of the ionic conductivity is better explained by variations in either the number of effective charge carriers or the ionic mobility.

II. MATERIALS AND METHODS

The samples were prepared following a two-step procedure. First, $AgPO_3$ was synthesized by mixing $(NH_4)_2HPO_4$ and $AgNO_3$ (*Sigma Aldrich*, purity > 99%). The powder mixture was homogenized in a mortar and melted in borosilicate (Pyrex®) crucibles at 770 K for 1h. Melt droplets were splat-quenched between stainless steel plates and several disks with approximately 1 mm thickness and 10 mm diameter were produced. The disks were homogeneous, colorless and transparent, with no bubbles. The second step consisted of

mixing the previously-made $AgPO_3$ in powder form with increasing molar fractions of a dopant salt (AgCl, AgBr or AgI - *Sigma Aldrich*, purity > 99% - from 10 to 50 mol%) and re-melting the batch as before, at 770 K for one hour in borosilicate crucibles.

For impedance spectroscopy, samples were prepared by sputtering thin gold electrodes on both surfaces using a Quorum QR150R ES Sputter equipment. The electric impedance was determined using a Solartron 1260 Impedance/Gain-Phase analyzer coupled with a Solartron 1296 Dielectric Interface system. Measurements were realized with a fixed voltage of 0.5 V and frequencies ranging from 1 to 10^6 Hz. During each run the temperature was controlled using a cryostat and a Novotherm furnace, with temperatures ranging from 170 to 410 K. Sample properties were extracted by modelling the experimental setup with a single parallel RC element representing the bulk glass as an ideal solid electrolyte[55,56] in series with a constant-phase element (CPE) representing the gold electrodes[57] (see **Figure 1**). The total impedance of this circuit is given by[57,58]:

$$Z^*(\omega) = Z' + i \cdot Z'' = Z^*_{RC} + Z^*_{CPE} = \frac{R - i \cdot \omega \cdot R^2 \cdot C}{1 + (\omega \cdot R \cdot C)^2} + \frac{1}{Q \cdot (i \cdot \omega)^{\alpha}} \quad 11$$

where i is the imaginary number, $\omega = 2\pi f$ is the angular frequency, R and C are the parameters of the RC element and Q and α the CPE parameters. From **Equation 11**, the complex modulus and the dc conductivity can be evaluated:

$$M^*(\omega) = M' + i \cdot M'' = i \cdot \omega \cdot C_0 \cdot Z^* \quad 12$$

$$\sigma_{dc} = \frac{1}{R} \cdot \frac{l}{A} \quad 13$$

where $C_0 = \epsilon_0 . (A/l)$ is the capacitance of the empty cell, ϵ_0 is the vacuum permittivity, l is the sample thickness and A is the sample area. Following **Equation 1**, the temperature dependence of the conductivity is given by the Arrhenius-scaling of both the number of effective charge carriers[17,59] and the ionic mobility[59]:

$$n(T) = n_c \cdot \exp\left(-\frac{E_n}{2 \cdot R \cdot T}\right) \quad (14)$$

$$\Gamma(T) = \Gamma_0 \cdot \exp\left(-\frac{E_m}{R \cdot T}\right) \quad (15)$$

where Γ_0 is the attempt frequency (in the order of the atomic vibration frequency of approximately 10^{13} s^{-1}), R is the universal gas constant, E_n and E_m are the activation energies for charge carrier creation and mobility, respectively. Substituting **Equations 14** and **15** in **Equation 10**:

$$\frac{\sigma_{\mathrm{dc}} \cdot T}{\Gamma(T)} = \frac{n(T) \cdot d^2 \cdot e^2}{g' \cdot k \cdot H_R} \quad (16)$$

$$\sigma_{dc} \cdot T = \frac{n_c \cdot d^2 \cdot e^2 \cdot \Gamma_0}{g' \cdot k \cdot H_R} \cdot \exp\left(-\frac{E_n}{2.R.T}\right) \cdot \exp\left(-\frac{E_m}{R.T}\right) \quad (17)$$

$$\sigma_{dc} \cdot T = \sigma_0 \cdot \exp\left(-\frac{E_\sigma}{RT}\right) \quad (18)$$

with

$$\sigma_0 = \frac{n_c \cdot d^2 \cdot e^2 \cdot \Gamma_0}{g' \cdot k \cdot H_R} \quad (19)$$

$$E_\sigma = \frac{E_n}{2} + E_m \quad (20)$$

III. RESULTS AND DISCUSSION

The impedance data measured for our samples is consistent with recently published literature[33,38,60], for example see **Figure 2**, for the Arrhenius graph of dc conductivity for the *x*AgI-(100-*x*)$AgPO_3$ glasses, and, as expected there is a marked decrease in activation energy with increasing iodide concentration.

For ion-conducting materials, the representation of experimental data by the complex electrical modulus formalism allows for access to dynamics of the mobile ions[46,54] from the analysis of the imaginary modulus $M'' = \mathrm{Im}(M^*)$ as a function of frequency, and has the advantage of being unaffected by electrode polarization[61,62]. For the silver halide – silver metaphosphate glasses the imaginary modulus as a function of frequency features a single, somewhat asymmetric peak. Scaling M'' and the frequency by M''_{max} and the peak frequency $f_{M''}$ collapses the data to a single "master" peak. The shape of this peak is nearly independent of temperature for each glass composition (**Figure 3 a)**) and the addition of halide salts progressively enhances the high-frequency tail, broadening the peak (**Figure 3 b)**). These results suggest that our samples share a common transport mechanism[63–65], namely the diffusive motion of silver ions. The peak broadening effect might reflect an increase in the number density of mobile ions[46,66]. However, the analysis of the electric modulus can be misleading, as the peak of the imaginary modulus could refer only to the dynamic response of the already mobile ions[1,29], instead of both the mobile and immobile ions.

The frequency of the imaginary modulus peak is used to scale the conductivity[67], but it is not the only frequency parameter used for scaling, and their choice is somewhat arbitrary[29,37,68]. Recently, Marple *et al*. have shown that the timescales of the dc to ac conductivity crossover frequency f^* (defined as the frequency that fulfils the relation $\sigma'(f^*) = 2.\sigma_{dc}$)[29,56] are associated with the diffusive hops of the mobile species between adjacent trapping sites[53], providing experimental evidence for the original concepts of Jonscher and Almond and West[54,56,69–71]. Comparing the temperature dependence of $f_{M''}$ and f^* and their activation energies with the activation energy of the conductivity in **Figure 4**, the activation energies of the peak of the imaginary modulus and the dc conductivity are equivalent (in agreement with previous reports on ionic conductors[56,69]), while the activation energy of the crossover frequency f^* is generally lower.

Since f^* is related to the ionic hopping frequency f_H [4,50–53,56,70], the Walden rule in **Equation 10** is satisfied by $\Gamma = f_H$. The Walden Plot in **Figure 5** shows that for all samples studied the

slope of the graph is very close to unity, as one would expect if the compositional dependence of the ionic conductivity was dominated by the ionic mobility. The relative clustering of the data, spreading only over approximately one order of magnitude along the $\log(\sigma_{\mathrm{dc}}.T)$ axis, indicates that the parameter $C' \propto \gamma.d^2.n_c/H_R$ is not strongly dependent on temperature and halide concentration, and therefore the number of effective charge carriers remains relatively constant in this system (assuming the Haven ratio is weakly dependent on temperature and composition[51]).

From **Equation 20** and the activation energies of dc conductivity and hopping frequency, the activation energy for charge carrier formation $E_n/2$ [17] can be estimated (see the inset in **Figure 6 a)**), and consequently the charge carrier number density for each glass composition can be calculated following **Equation 14**. Values of n ranging from 3.4×10^{20} to 1.4×10^{22} ions.cm^{-3} (indicating that $0.02 \leq \gamma \leq 0.89$) are in agreement with previous NMR and Impedance Spectroscopy studies[3,35] and with the clustering of the data shown in **Figure 5**, meaning that for this glass system a substantial fraction of the number of silver ions contributes actively to the measured conductivity (**Figure 6 a)**). This is in contrast to the "weak electrolyte" approach, where the conductivity should be governed by the increase in the fraction of mobile charge carriers γ[17]. Another variable that affects the fraction of mobile ions is the timescale involved. Following ergodicity arguments, as the timescale tends to infinity, all ions contribute to the conductivity and the number density of mobile ions becomes equal to the total number density of ions (and, consequently, $\gamma \rightarrow 1$). Thus, the characterization of γ only makes sense when it refers to a particular time-scale[4], which is $t_H = 1/f_H$ in our analysis.

Substituting the values of the number density of mobile ions in **Equation 1** allows for the estimation of the ionic mobility (**Figure 6 b)**), and the range of values (from $\sim 4 \times 10^{-13}$ m^2.V^{-1}.s^{-1} for $AgPO_3$ up to $\sim 7 \times 10^{-9}$ m^2.V^{-1}.s^{-1} for 50AgI - 50$AgPO_3$ at 298 K) are also in agreement with NMR estimates[35]. The mobility seems to be strongly affected by the type of halide salt incorporated in silver metaphosphate, with $\mu_{\mathrm{AgI}} > \mu_{\mathrm{AgBr}} > \mu_{\mathrm{AgCl}}$, decreasing with increasing halide field strength.

IV. CONCLUSION

Silver halide – silver metaphosphate glass samples were synthesized and characterized via Impedance Spectroscopy. These glasses follow the so-called “canonical scaling”, and therefore a graph of $\log(\sigma_{\mathrm{dc}}.T) \times \log f_H$ shows a slope of unity, indicating that the conductivity is dominated by ionic mobility. The clustering of the data points indicates that the number density of effective charge carriers does not change substantially with increasing halide concentration, which is in agreement with the activation energy analysis. Therefore the enhancement in the ionic conductivity observed by the addition of halide salts can be attributed to the increased mobility of the silver ions in the glassy matrix.

ACKNOWLEDGEMENTS

The authors would like to thank C. B. Bragatto and A. C. M. Rodrigues for their experimental help and invaluable discussions. The financial support of the German Science Foundation through its priority program SPP 1594 (project number WO 1220/10-1), the European Research Council under the EU’s Horizon 2020 research and innovation program (ERC grant UTOPES, grant agreement number 681652), and the Australian Research Council (grant number DP170104367).

BIBLIOGRAPHY

1. Angell, C. A. Mobile ions in amorphous solids. *Annu. Rev. Phys. Chem.* **43,** 693–717 (1992).

2. Cutroni, M., Mandanici, A., Mustarelli, P., Tomasi, C. & Federico, M. Ionic conduction and dynamical regimes in silver phosphate glasses. *J. Non-Cryst. Solids* **307–310,** 963–970 (2002).

3. Bhattacharya, S. & Ghosh, A. Conductivity spectra in fast ion conducting glasses: Mobile ions contributing to transport process. *Phys. Rev. B* **70,** 172203 (2004).

4. Dyre, J. C., Maass, P., Roling, B. & Sidebottom, D. L. Fundamental questions relating

to ion conduction in disordered solids. *Reports Prog. Phys.* **72,** 46501 (2009).

5. Mauro, J. C. & Zanotto, E. D. Two Centuries of Glass Research: Historical Trends, Current Status, and Grand Challenges for the Future. *Int. J. Appl. Glas. Sci.* **5,** 313–327 (2014).

6. Kim, J. G. *et al.* A review of lithium and non-lithium based solid state batteries. *J. Power Sources* **282,** 299–322 (2015).

7. Doreau, M., Malugani, J. P. & Robert, G. Verres mixtes AgPO3-NaI et AgPO3-KI. Domaine vitreux, conductivite electrique, approche structurale. *Electrochim. Acta* **26,** 711–717 (1981).

8. Malugani, J. P., Mercier, R., Fahys, B. & Robert, G. Ionic Conductivity of and Raman Spectroscopy Investigation Binary Oxosalts (1-x)AgPO3-xAg2SO4 Glasses. *J. Solid State Chem.* **45,** 309–316 (1982).

9. Martin, S. W. Ionic Conduction in Phosphate Glasses. *J. Am. Ceram. Soc.* **74,** 1767–1784 (1991).

10. Martin, S. W. & Schiraldi, A. Glass Formation and High Conductlvlty In the Ternary System AgI + AgAsO4 + AgPO3: Host to Glassy AgI? *J. Phys. Chem.* **89,** 2070–2076 (1985).

11. Malugani, J. P., Mercier, R. & Tachez, M. Correlation between structural and electrical properties in (1-x)AgPO3.xMX2 glasses (M = Pb2+, Hg2+; X = I-, Br-, Cl-) from Raman spectroscopy and ionic conductivity measurements. *Solid State Ionics* **21,** 131–138 (1986).

12. Scotti, S., Villa, M., Mustarelli, P. & Cutroni, M. Structure, conductivity and acoustic attenuation in (Ag2SO4)x(AgPO3)1-x. *Solid State Ionics* **53–56,** 1237–1244 (1992).

13. Cutroni, M., Magistris, A. & Villa, M. Dynamics and structure of (Ag2S)x(AgPO3)1-x glasses studied by ultrasounds and 31P NMR. *Solid State Ionics* **53–56,** 1232–1236

(1992).

14. Kartini, E. *et al.* Structural , thermal and electrical properties of AgI-Ag2S-AgPO3 superionic glasses. *J. Non-Cryst. Solids* **312–314,** 628–632 (2002).

15. Niiya, N., Wakamura, K. & Takahashi, H. Concentration and temperature dependences of infrared reflectivity spectra in glass ionic conductor AgI- and Ag2X-AgPO3 systems (X = S, Se, Te). *Solid State Ionics* **177,** 659–668 (2006).

16. Thieme, A. *et al.* Structure and properties of alkali and silver sulfophosphate glasses. *J. Non-Cryst. Solids* **410,** 142–150 (2015).

17. Rodrigues, A. C. M., Nascimento, M. L. F., Bragatto, C. B. & Souquet, J. L. Charge carrier mobility and concentration as a function of composition in AgPO3-AgI glasses. *J. Chem. Phys.* **135,** 234504 (2011).

18. Tachez, M., Mercier, R., Malugani, J. P. & Dianoux, A. J. Quasielastic and inelastic neutron scattering from AgPO3-AgI glass. *Solid State Ionics* **20,** 93–98 (1986).

19. Tachez, M., Mercier, R., Malugani, J. P. & Chieux, P. Structure determination of AgPO3 and (AgPO3)0.5(AgI)0.5 glasses by neutron diffraction and small angle neutron scattering. *Solid State Ionics* **25,** 263–270 (1987).

20. Malugani, J. P. & Mercier, R. Vibrational properties of and short range order in superionic glasses AgPO3-AgX (X = I, Br, Cl). *Solid State Ionics* **13,** 293–299 (1984).

21. Ingram, M. D. Ionic conductivity and glass structure. *Philos. Mag. B* **60,** 729–740 (1989).

22. Kartini, E. *et al.* Anomalous temperature dependence of the first diffraction peak in the superionic glass (AgI)x(AgPO3)1-x. *Phys. Rev. B* **61,** 1036–1042 (2000).

23. Vogel, M., Brinkmann, C., Eckert, H. & Heuer, A. Silver dynamics in silver iodide/silver phosphate glasses studied by multi-dimensional 109Ag NMR. *Phys. Chem. Chem. Phys.* **4,** 3237–3245 (2002).

24. Mustarelli, P., Linati, L., Tartara, V., Tomasi, C. & Magistris, A. Structure/transport relationships in silver-based oxide glasses: 1-D and 2-D NMR information. *Solid State Nucl. Magn. Reson.* **27,** 112–121 (2005).

25. Ren, J. & Eckert, H. Anion distribution in superionic Ag3PO4-AgI glasses revealed by dipolar solid state NMR. *J. Phys. Chem. C* **117,** 24746–24751 (2013).

26. Rodrigues, B. P. & Wondraczek, L. Medium-range topological constraints in binary phosphate glasses. *J. Chem. Phys.* **138,** 244507 (2013).

27. Rao, K. J. *Structural Chemistry of Glasses*. (Elsevier Science, 2002).

28. Bandara, T. M. W. J. & Mellander, B.-E. in *Ionic Liquids: Theory, Properties, New Approaches* (ed. Kokorin, A.) 384–407 (Intech, 2011). doi:10.5772/603

29. Roling, B., Happe, A., Funke, K. & Ingram, M. D. Carrier concentrations and relaxation spectroscopy: New information from scaling properties of conductivity spectra in ionically conducting glasses. *Phys. Rev. Lett.* **78,** 2160–2163 (1997).

30. Roling, B., Happe, A., Ingram, M. D. & Funke, K. Interrelation between different mixed cation effects in the electrical conductivity and mechanical loss spectra of ion conducting glasses. *J. Phys. Chem. B* **103,** 4122–4127 (1999).

31. Souquet, J. L. Electrochemical properties of ionically conductive glasses. *Solid State Ionics* **5,** 77–82 (1981).

32. Souquet, J. L. & Perera, W. G. Thermodynamics applied to ionic transport in glasses. *Solid State Ionics* **40–41,** 595–604 (1990).

33. Bragatto, C. B., Rodrigues, A. C. M. & Souquet, J. L. Dissociation Equilibrium and Charge Carrier Formation in AgI-AgPO3 Glasses. *J. Phys. Chem. C* **121,** 13507–13514 (2017).

34. Clement, V., Ravaine, D., Deportes, C. & Billat, R. Measurement of Hall mobilites in

AgPO3-AgI glasses. *Solid State Ionics* **28–30,** 1572–1578 (1988).

35. Mustarelli, P., Tomasi, C., Magistris, A. & Linati, L. Carrier density and mobility in AgI-AgPO3 glasses: A NMR study. *Phys. Rev. B* **63,** 144203 (2001).

36. Kabi, S. & Ghosh, A. Dynamics of Ag+ ions and immobile salt effect in CdI2 doped silver phosphate glasses. *Solid State Ionics* **187,** 39–42 (2011).

37. Kabi, S. & Ghosh, A. Ion dynamics in glassy ionic conductors: Scaling of mean square displacement of mobile ions. *Europhys. Lett.* **108,** 36002 (2014).

38. Singh, D. P., Shahi, K. & Kar, K. K. Superlinear frequency dependence of AC conductivity and its scaling behavior in xAgI-(1-x)AgPO3 glass superionic conductors. *Solid State Ionics* **287,** 89–96 (2016).

39. Angell, C. A., Ansari, Y. & Zhao, Z. Ionic Liquids: Past, present and future. *Faraday Discuss.* **154,** 9–27 (2012).

40. Schreiner, C., Zugmann, S., Hartl, R. & Gores, H. J. Fractional walden rule for ionic liquids: Examples from recent measurements and a critique of the so-called ideal KCl line for the Walden plot. *J. Chem. Eng. Data* **55,** 1784–1788 (2010).

41. Murch, G. E. & Dyre, J. C. Correlation effects in ionic conductivity. *Crit. Rev. Solid State Mater. Sci.* **15,** 345–365 (1989).

42. Murch, G. E. The exact Nernst-Einstein equations and the interpretation of cross phenomenological coefficients in unary, binary, and ambipolar systems. *Radiat. Eff.* **73,** 299–305 (1983).

43. Xu, W. & Angell, C. A. Solvent-free electrolytes with aqueous solution-like conductivities. *Science* **302,** 422–425 (2003).

44. Yoshizawa, M., Xu, W. & Angell, C. A. Ionic Liquids by Proton Transfer: Vapor Pressure, Conductivity, and the Relevance of DpKa from Aqueous Solutions. *J. Am. Chem. Soc.*

125, 15411–15419 (2003).

45. Nitta, K., Nohira, T., Hagiwara, R., Majima, M. & Inazawa, S. Physicochemical properties of ZnCl2-NaCl-KCl eutectic melt. *Electrochim. Acta* **54,** 4898–4902 (2009).

46. Angell, C. A. Dynamic processes in ionic glasses. *Chem. Rev.* **90,** 523–542 (1990).

47. Ngai, K. L. A review of critical experimental facts in electrical relaxation and ionic diffusion in ionically conducting glasses and melts. *J. Non-Cryst. Solids* **203,** 232–245 (1996).

48. *Dynamics of Glassy, Crystalline and Liquid Ionic Conductors*. (Springer International Publishing, 2017). doi:10.1007/978-3-319-42391-3

49. Sidebottom, D. L., Green, P. F. & Brow, R. K. Brillouin scattering in alkali metaphosphate glasses and melts. *J. Mol. Struct.* **479,** 219–226 (1999).

50. Sidebottom, D. L. Dimensionality dependence of the conductivity dispersion in ionic materials. *Phys. Rev. Lett.* **83,** 983–986 (1999).

51. Sangoro, J. R. & Kremer, F. Charge Transport and Glassy Dynamics in Ionic Liquids. *Acc. Chem. Res.* **45,** 525–532 (2012).

52. Shaw, A. & Ghosh, A. Correlation of microscopic length scales of ion dynamics with network structure in lithium-iodide-doped lithium metaphosphate glasses. *Europhys. Lett.* **100,** 66003 (2012).

53. Marple, M. A. T., Avila-Paredes, H., Kim, S. & Sen, S. Atomistic interpretation of the ac-dc crossover frequency in crystalline and glassy ionic conductors. *J. Chem. Phys.* **148,** 204507 (2018).

54. Sidebottom, D. L. Understanding ion motion in disordered solids from impedance spectroscopy scaling. *Rev. Mod. Phys.* **81,** 999–1014 (2009).

55. Hodge, I. M., Ingram, M. D. & West, A. R. Impedance and modulus spectroscopy of

polycrystalline solid electrolytes. *J. Electroanal. Chem.* **74,** 125–143 (1976).

56. Almond, D. P. & West, A. R. Impedance and modulus spectroscopy of 'real' dispersive conductors. *Solid State Ionics* **11,** 57–64 (1983).

57. *Impedance Spectroscopy: Theory, Experiment, and Applications*. (Wiley-Interscience, 2005). doi:10.1002/0471716243

58. Lvovich, V. F. *Impedance Spectroscopy - Aplications to Electrochemical and Dielectric Phenomena*. (John Wiley & Sons, 2012).

59. Hairetdinov, E. F., Uvarov, N. F., Patel, H. K. & Martin, S. W. Estimation of the free-charge-carrier concentration in fast-ion conducting Na2S-B2S3 glasses from an analysis of the frequency-dependent conductivity. *Phys. Rev. B* **50,** 13259–13266 (1994).

60. Palles, D., Konidakis, I., Varsamis, C. P. E. & Kamitsos, E. I. Vibrational spectroscopic and bond valence study of structure and bonding in A2O3-containinig AgI-AgPO3 glasses. *RSC Adv.* **6,** 16697–16710 (2016).

61. Howell, F. S., Bose, R. A., Macedo, P. B. & Moynihan, C. T. Electrical relaxation in a glass-forming molten salt. *J. Phys. Chem.* **78,** 639–648 (1974).

62. Dyre, J. C. The random free-energy barrier model for ac conduction in disordered solids. *J. Appl. Phys.* **64,** 2456–2468 (1988).

63. Karlsson, C., Mandanici, A., Matic, A., Swenson, J. & Boerjesson, L. Dielectric modulus analysis of mixed alkali LixRb1-xPO3 glasses. *J. Non-Cryst. Solids* **307–310,** 1012–1016 (2002).

64. Bhide, A. & Hariharan, K. Sodium ion transport in NaPO3-Na2SO4 glasses. *Mater. Chem. Phys.* **105,** 213–221 (2007).

65. Gowda, V. C. V, Reddy, C. N. & Rao, K. J. A new approach for understanding ion

transport in glasses; Example of complex alkali diborate glasses containing lead, bismuth and tellurium oxides. *Bull. Mater. Sci.* **36,** 71–85 (2013).

66. Sidebottom, D. L., Roling, B. & Funke, K. Ionic conduction in solids: Comparing conductivity and modulus representations with regard to scaling properties. *Phys. Rev. B* **63,** 24301 (2001).

67. Patel, H. K. & Martin, S. W. Fast ionic conduction in Na2S+B2S3 glasses: Compositional contributions to nonexponentiality in conductivity relaxation in the extreme low-alkali-metal limit. *Phys. Rev. B* **45,** 10292–10300 (1992).

68. Sidebottom, D. L. Universal approach for scaling the ac conductivity in ionic glasses. *Phys. Rev. Lett.* **82,** 3653–3656 (1999).

69. Almond, D. P., Hunter, C. C. & West, A. R. The extraction of ionic conductivities and hopping rates from a.c. conductivity data. *J. Mater. Sci.* **19,** 3236–3248 (1984).

70. Almond, D. P., Duncan, G. K. & West, A. R. The determination of hopping rates and carrier concentrations in ionic conductors by a new analysis of ac conductivity. *Solid State Ionics* **8,** 159–164 (1983).

71. Popov, I. I., Nigmatullin, R. R., Khamzin, A. A. & Lounev, I. V. Conductivity in disordered structures: Verification of the generalized Jonscher's law on experimental data. *J. Phys. Conf. Ser.* **394,** 12026 (2012).

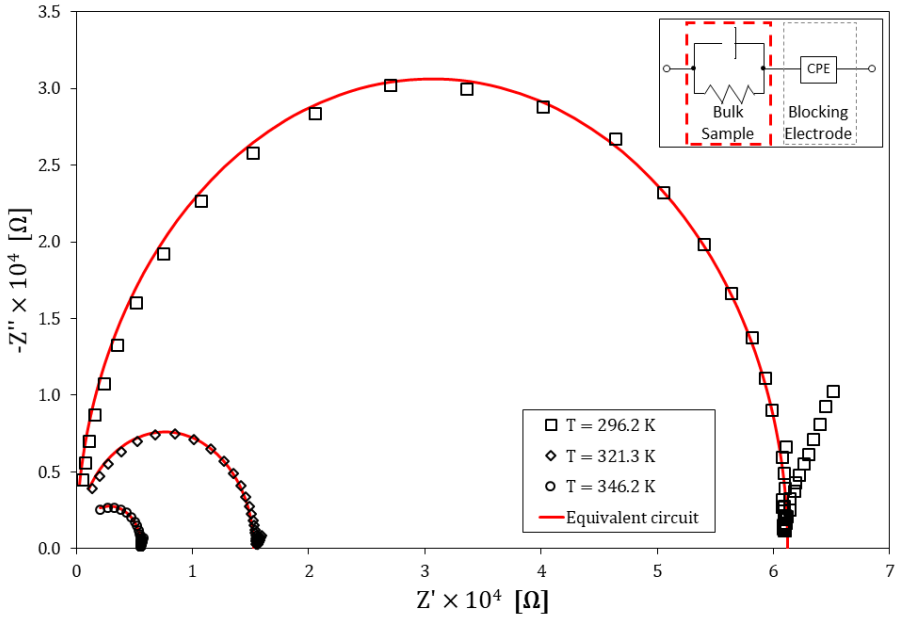

Figure 1. Nyquist plot of the complex impedance measured for the 90AgPO3-10AgI sample in different temperatures. The empty symbols show the experimental data and the continuous lines represent the response of the equivalent circuit as shown in the inset.

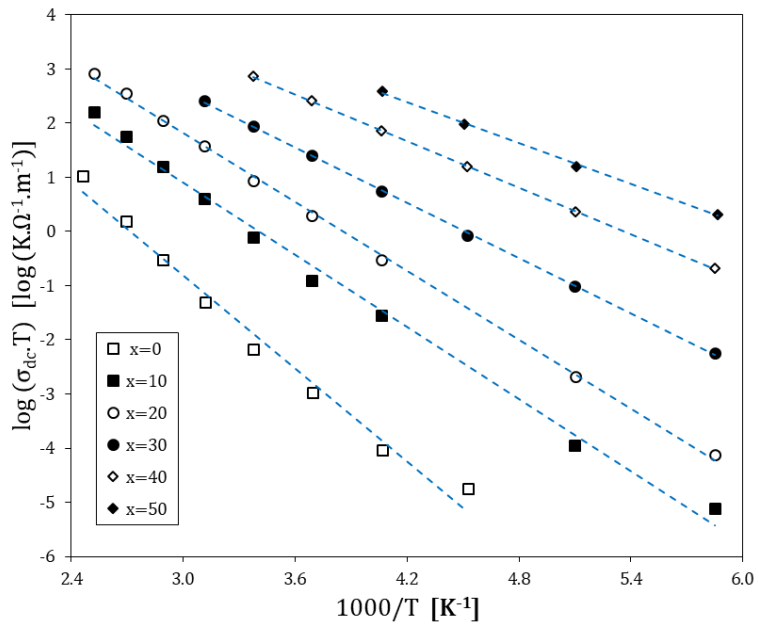

Figure 2. Arrhenius plot of the dc conductivity as a function of temperature for the xAgI-(100-x)$AgPO_3$ glass system, the dashed lines are linear fits of the data and the error bars are smaller than the size of the data points.

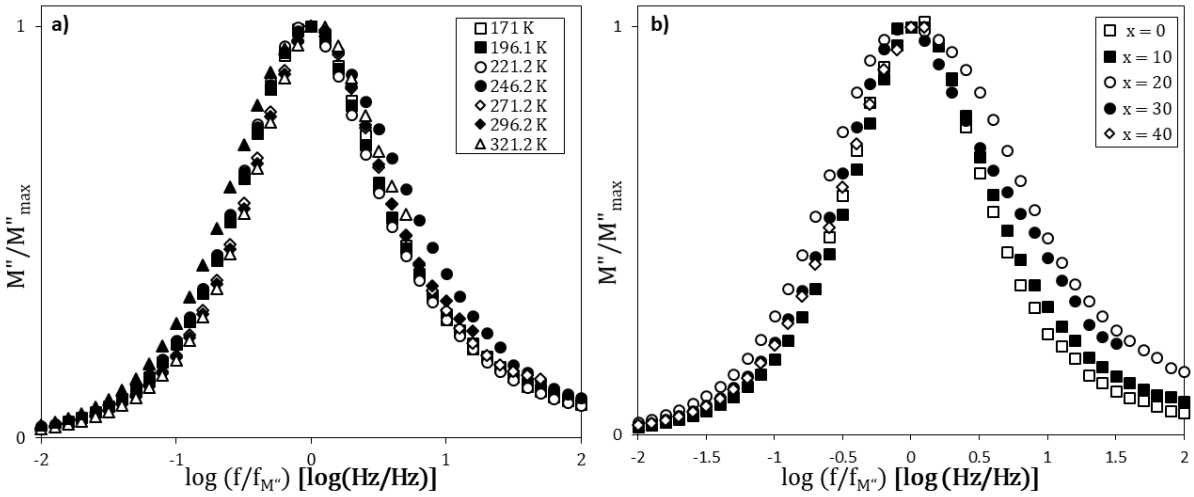

Figure 3. Scaled plots of the Imaginary modulus as a function of frequency. **a)** with increasing temperature for 30AgCl-70$AgPO_3$ glass; **b)** with increasing halide content for xAgBr-(100-x)$AgPO_3$ glasses at 271 K.

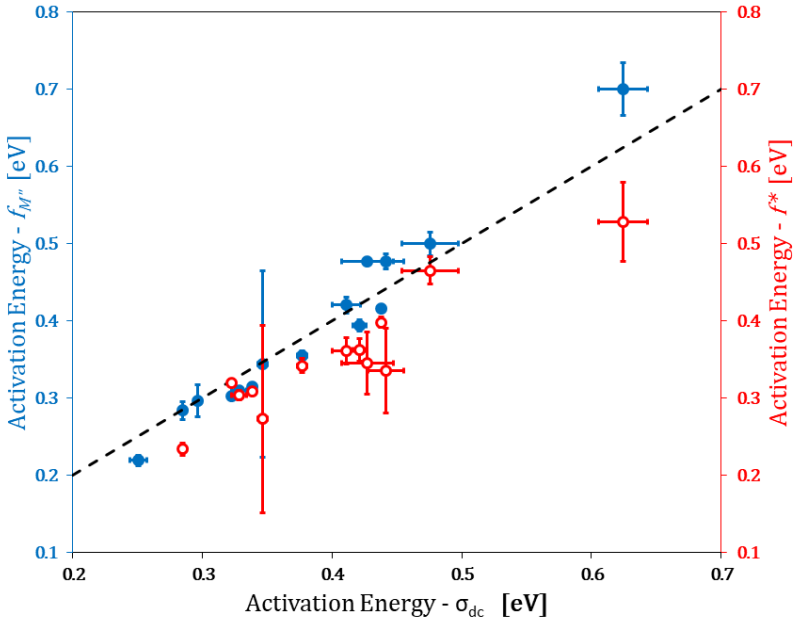

Figure 4. Activation energies of the imaginary modulus peak frequency $f_{M''}$ (filled symbols) and the crossover frequency f^* (empty symbols) compared to the activation energy of dc conductivity σ_{dc}. The dashed line illustrates a 1:1 ratio.

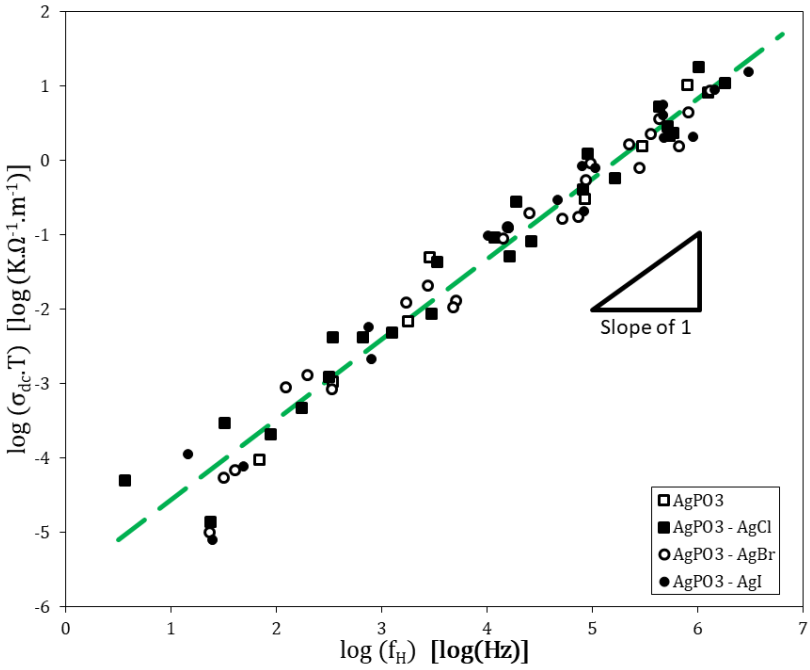

Figure 5. Walden Plot following **Equation 10** for the measured samples. The dashed line is the linear regression of the data, resulting in a slope of 1.08 ± 0.02.

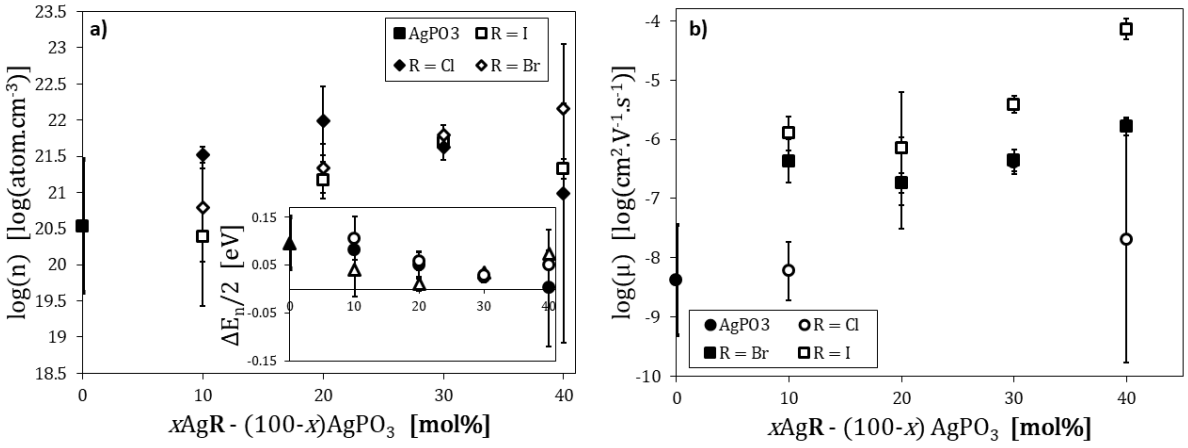

Figure 6. **a)** Number density of effective charge carrier at 298 K as a function of composition, and the inset shows the compositional dependence of the activation energy for charge carrier creation; and, **b)** calculated ionic mobility at 298 K as a function of composition.